

East, K., "National Engineering Laboratory Steam Tables", H. M. Stationary Office, Edinburgh, Scotland (1964).

Flory, P. J., "Thermodynamics of Polymer Solutions," *Disc. Faraday Soc.*, **49**, 7 (1970).

Goodwin, R. D., "Thermophysical Properties of Methane, from 90 to 500°K at Pressures to 700 bars," *NBS Tech. Note* 653 (1974).

Gosman, A. L., R. D. McCarthy, and J. G. Hust, "Thermodynamic Properties of Argon From the Triple Point to 300°K at Pressures to 1000 atm." National Standard Reference Data Series (NBS), No. 27 (1969).

Hijmans, J., "Phenomenological Formulations of the Principle of Corresponding States for Liquids Consisting of Chain Molecules," *Physica*, **27**, 433 (1961).

Hill, T. L., *Introduction to Statistical Thermodynamics*, p. 286, Addison-Wesley, Reading, Mass. (1962).

Jacobsen, R. T., R. B. Stewart, R. D. McCarty, and H. J. M. Hanley, "Thermophysical Properties of Nitrogen From the Fusion Line to 3500°R for Pressures to 15000 Psia," *NBS Tech. Note* 648 (1973).

Levelt-Senger, J. M. H., "From van der Waals Equation to Scaling Laws," *Physica*, **73**, 73 (1974).

Lewis, G. N., M. Randall, K. S. Pitzer, and L. Brewer, *Thermodynamics*, 2 ed., Appendix 1, McGraw-Hill, New York (1961).

Patterson, D., and G. Delmas, "Corresponding States Theories and Liquid Models," *Disc. Faraday Soc.*, **49**, 98 (1970).

Prigogine, I., *The Molecular Theory of Solutions*, North Holland Publishing Co., Amsterdam (1957).

Redlich, O., and J. N. S. Kwong, "On the Thermodynamics of Solutions V," *Chem. Rev.*, **44**, 233 (1949).

Reed, T. M., and K. E. Gubbins, *Applied Statistical Mechanics*, McGraw-Hill, New York (1973).

Rowlinson, J. S., "The Thermodynamics of the Critical Point in One-Component Systems," *Ber. Bunsen-Ges. Phys. Chem.*, **76**, 281 (1972).

Soave, G., "Equilibrium Constants from a Modified Redlich-Kwong Equation of State," *Chem. Eng. Sci.*, **27**, 1197 (1972).

Vera, H. J., and J. M. Prausnitz, "Interpretative Review. Generalized van der Waals Theory for Dense Fluids," *Chem. Eng. J.*, **3**, 1 (1972).

Manuscript received April 23, 1975; revision received June 27, and accepted July 8, 1975.

APPENDIX

The molecular-dynamic results of Alder are given in a form where the Holmholtz energy is the sum of a hard-sphere part and a perturbation part; the latter follows from attractive intermolecular forces. These are represented by a square-well

potential where the width of the well is a fixed multiple ($\frac{1}{2}$) of the hard-sphere diameter. For the hard-sphere part we use the Carnahan-Starling equation. For the perturbation part we use Alder's results:

$$W(\tilde{T}, \tilde{v}) = \sum_{n=1}^4 \sum_{m=1}^M \left(\frac{A_{nm}}{\tilde{v}^m} \right) \left(\frac{1}{\tilde{T}^{n-1}} \right) \quad (A1)$$

The dimensionless constants A_{nm} are

$$\begin{aligned} A_{11} &= -7.0346 \\ A_{12} &= -7.2736 \\ A_{13} &= -1.2520 \\ A_{14} &= 6.0825 \\ A_{15} &= 6.8 \\ A_{16} &= 1.7 \\ A_{21} &= -0.33015580 \times 10^1 \\ A_{22} &= -0.98155782 \times 10^0 \\ A_{23} &= +0.22022115 \times 10^3 \\ A_{24} &= -0.19121478 \times 10^4 \\ A_{25} &= +0.86413158 \times 10^4 \\ A_{26} &= -0.22911464 \times 10^5 \\ A_{27} &= +0.35388809 \times 10^5 \\ A_{28} &= -0.29353643 \times 10^5 \\ A_{29} &= +0.10090478 \times 10^5 \\ A_{31} &= -0.11868777 \times 10^1 \\ A_{32} &= +0.72447507 \times 10^1 \\ A_{33} &= -0.17432407 \times 10^2 \\ A_{34} &= +0.19666211 \times 10^2 \\ A_{35} &= -0.85145188 \times 10^1 \\ A_{41} &= -0.51739049 \times 10^0 \\ A_{42} &= +0.25259812 \times 10^1 \\ A_{43} &= -0.41246808 \times 10^1 \\ A_{44} &= +0.23434564 \times 10^1 \end{aligned}$$

When

$$\begin{aligned} n &= 1, & M &= 6 \\ n &= 2, & M &= 9 \\ n &= 3, & M &= 5 \\ n &= 4, & M &= 4 \end{aligned}$$

For methane the effect of temperature on v_{sp}^* is given by

$$\begin{aligned} v_{sp}^* &= 1.467662 - 1.504333\tilde{T} + 2.695236\tilde{T}^2 - 2.046844\tilde{T}^3 \\ &+ 0.8062849\tilde{T}^4 - 0.1735586\tilde{T}^5 + 0.019398\tilde{T}^6 - 0.0008816\tilde{T}^7 \end{aligned}$$

where subscript sp (specific) indicates that v^* is per gram.

The Decomposition Kinetics of Molybdenite in an Argon Plasma

A reactor system was developed for the study of heterogeneous reaction kinetics in plasma tail flames. This system was used to investigate the thermal decomposition kinetics of stationary particles of molybdenum disulfide in both the molten and solid state when exposed to argon flames in the temperature range 3 000°K to 8 000°K.

In the solid state a shrinking-core reaction model was obeyed. The rate of reaction was largely controlled by the diffusion of sulfur vapor outwards through the product layer. An apparent activation energy of 134

R. J. MUNZ and W. H. GAUVIN
McGill University, Montreal, Quebec, Canada

R. J. Munz is with Noranda Research Centre, Pointe-Claire, Quebec, Canada.

kcal/mole was calculated for the particle temperature range 1 613° to 1 833°K. The molten state reaction was controlled by the rate of heat transfer to the reacting particle. Calculations indicated that the rate of heat transfer was influenced by the efflux of sulfur.

SCOPE

Since the early 1960's, increasing attention has been devoted to the use and potential of plasmas as chemical reactors. Sayce (1972) has given a comprehensive review of plasma technology and its applications to extractive metallurgy. Although plasma generators capable of continuous operation at several megawatts are commercially available, the use of plasmas as chemical reactors on a commercial scale is limited to three processes: the production of acetylene, that of titanium oxide, and the dissociation of zircon sand into zirconia and silica. Of these, only the last makes use of solid feed material. Waldie (1972a) has reviewed the use of plasmas for such physical treatments as plasma spraying, spheroidizing, and the production of ultrafine particles and for such reactions as metallurgical extraction and the production of refractory carbides and nitrides. In spite of the large number of patents which have resulted from the latter activities, no commercial processes have been developed, other than those listed above, to the authors' knowledge. Plasma processing must at present be limited to products whose high market value offsets the high cost of plasma operation. Moreover, the

recent review of Waldie (1972b) on particle dynamics and transport phenomena in plasmas emphasizes the fact that more fundamental knowledge is required for process design.

The thermal decomposition of molybdenite (MoS_2) into molybdenum metal and elemental sulfur is a promising candidate for plasma processing. The current method of production is not only circuitous but produces sulfur dioxide as a pollutant and leaves some oxide in the final product. The decomposition in vacuum was shown by Scholz et al. (1961) to be feasible but was limited to batch operation, and the high temperatures involved presented containment problems. Conversions of up to 70% were achieved by Huska and Clump (1967) and by Charles et al. (1970) in argon induction plasmas.

The objectives of the present work were twofold: to develop a facility which could be used for the study of a variety of heterogeneous reactions in a plasma atmosphere and to obtain kinetic data for the thermal decomposition of molybdenite in an argon plasma.

CONCLUSIONS AND SIGNIFICANCE

One of the major objectives of this study was to design a reactor system which would allow the measurement of reaction kinetic data for a wide variety of heterogeneous reactions in a plasma flame. The system had to meet a number of requirements, chief among which was to minimize both the particle heating up period and its subsequent quenching, while permitting visual observations and rigid control of operating conditions. Axial and radial temperature gradients in both the gas and reacting particles were minimized by using a particle size which was small relative to the plasma jet diameter.

The reactor was used to investigate the thermal decomposition of both solid and molten molybdenum disulfide in an argon plasma tail flame. This is believed to be the first comprehensive study of heterogeneous chemical kinetics in a nontransferred plasma flame. It has been shown that for the solid state reaction, the time taken for complete conversion of spheres may be calculated with reasonable accuracy on the basis of a single-stage, shrinking-core model provided that the particle diameter, void fraction, and temperature are known. This model assumes that the rate of reaction is controlled by the diffusion of sulfur through the product layer. The general correlation of Equation (7) is proposed in conjunction with the effective diffusivity represented in Equation (10). For practical purposes, the kinetic data obtained with spherical pellets can easily be applied to other sample geometries such as cylindrical shapes or rectangular briquettes.

In the case of the injection of fine powdered particles (as naturally produced in the flotation concentration process) directly into hotter regions of the plasma tail flame, a much different situation would prevail. In the first place, much lower particle Reynolds numbers would be obtained. For example, at a mean film temperature of 6 000°K, the Reynolds number of a particle with a diameter of 20 μ , moving at a relative velocity of 5 m/s, would only be 4×10^{-2} , as opposed to values near 100 obtained in the

present work. Since the fine disklike natural molybdenite particles present a much higher surface area-to-volume ratio than the stationary spheres which were reacted here, it would be expected that the greatest part of the solid state reaction of freely entrained powder would be governed by the mass transfer of sulfur vapor from the reacting particle surface. This would lead to predicted Sherwood numbers close to 2.

The liquid state reaction was found to be governed by the rate of heat transfer to the reacting particles. This conclusion is particularly significant in that the conversion of finely divided particles injected into an inert plasma can now be computed with reasonable confidence, provided that the plasma flow field and geometry have been established. Two such studies have been completed by Boulos and Gauvin (1974) and Bhattacharyya and Gauvin (1974). These simulations may be used to great advantage to optimize the design of a plasma reactor and particle injection conditions.

The measured rates of reaction were used to calculate the rates of heat consumption by the reaction. These compared to the rate of convective heat transfer to the particles, by using the theoretical predictions of Hoffman and Ross (1972) and the temperature and velocity profiles predicted by Boulos and Gauvin (1974). Mean plasma temperatures were measured by using a calorimeter designed and constructed for this work. The calculations agreed well with the theoretical predictions. Moreover, they pointed out the importance of mass transfer on heat transfer in a reacting plasma system.

The reactor system used in this work will be capable of providing more complete information on heat and mass transfer once local velocities and turbulence characteristics in the plasma tail flame have been determined by laser doppler anemometry. This work is currently in progress in these laboratories.

The study of heterogeneous kinetics in plasma flames has received little attention so far, in spite of the fact that no other reaction system will closely simulate plasma conditions. Triché et al. (1968) studied the vaporization and carburization of a number of oxides in an induction flame. The progress of the reactions was followed spectroscopically, but no attempt was made to vary the temperature of the reacting particles.

The only other reported kinetic studies in a plasma flame are those of Matsumoto and co-workers (Matsumoto, 1968, 1969; Matsumoto and Kawai, 1972). The main objective of these studies was the synthesis of refractory metal nitrides and oxides in a transferred arc, although some kinetic data were presented. In all cases, the reacting samples rested on a water-cooled support and so exhibited enormous thermal gradients.

Maru et al. (1969a,b) studied the kinetics of decomposition of both MoS_2 and Mo_2S_3 (a reaction intermediate) up to a temperature of 1700°K in a vacuum thermal balance. The rate of reaction was found to be controlled by the diffusion of sulfur through the product layer, and a shrinking core model was found to apply to the reaction. No data on the decomposition kinetics are available at temperatures above 1700°K or in a plasma system. Since the mineral is known to undergo melting with decomposition (Zelikman and Belyaevskaya, 1956) at a temperature of about 1920°K , a study of the decomposition in a plasma flame in both the solid and liquid states is a definite requisite to the successful design of a plasma process based on the decomposition reaction.

The molybdenum disulfide decomposition reaction is strongly endothermic, and it would be expected that the transfer of heat to the particle from the plasma surroundings would play a major role in the liquid state reaction kinetics. The subject of heat transfer to particles in plasmas has recently been reviewed by Waldie (1972 b), and heat transfer to spheres has been reviewed by Kubanek et al. (1968) and by Katta and Gauvin (1973a). These reviews have made it abundantly clear that solids-gas heat transfer in plasma surroundings exhibit unique characteristics which shall now be summarized.

PURE HEAT TRANSFER

First of all, it is advisable to differentiate the behavior of small particles from that of large particles. In the case of small particles entrained by a plasma stream, the motion is characterized by a very low Reynolds number (and hence Peclet number) generally less than 1. Forced convection heat transfer will therefore be negligible, and so will the effect of plasma turbulence, except insofar as the particle may traverse eddies of different temperatures. Conduction heat transfer will predominate. Radiation heat transfer from the particles to the boundaries of the system will also be important, while that of the optically thin plasma to the particle will be negligible. In the case of large particles (say 1 mm and up), whether stationary or fluid conveyed, Reynolds number is now significant (50 and higher), and forced convection and turbulence effects will now become important, in addition, of course, to the radiation effects. In both cases, the picture is further complicated by two phenomena which are characteristics of these systems, namely recombination effects and the high temperature gradients surrounding the particles. These two effects will now be discussed in turn.

Concerning recombination effects, it is well known that as the plasma approaches a cold particle or surface, the dissociated and ionized species recombine on the latter, resulting in a higher apparent rate of heat transfer. This was observed by Chludzinski et al. (1965), Kimura and

Kanzawa (1965), and Petrie (1969). The argon plasma tail flames used in this work, however, reached only about 8000°K . At this temperature, ionization is small, and thus recombination effects may be ignored. The same conclusion applies to high energy metastables, such as 1S_5 and 1S_3 argon metastables in the case of an argon plasma (Johnston, 1971).

Concerning the high temperature gradients surrounding the particle, the difference in temperature between the plasma and the surface of the particle can easily amount to several thousand degrees Kelvin. Gas properties will therefore vary tremendously in the vicinity of the particle, and it becomes difficult to choose a proper reference temperature for the evaluation of the relevant fluid properties in the differential equations of energy transfer.

From the works of Kubanek et al. (1968), Rother et al. (1968a,b), and Katta and Gauvin (1973a,b) it would appear that correlations based on bulk gas temperatures have been more successful for large stationary particles at high levels of turbulence. For smaller particles, in laminar flow, the use of a mean film temperature is more correct.

EFFECT OF MASS TRANSFER

The superposition of mass transfer in particulate systems will affect the other two transport phenomena. This will occur upon vaporization of the particle (or of one of its constituents), or upon gas evolution as a result of chemical reaction and/or decomposition. An experimental study of the effect of mass transfer on the momentum transfer of freely moving particles in turbulent motion has been reported by Clamen and Gauvin (1968). In the case of heat transfer, Bonet (1974) has recently presented a detailed analysis of the effects of evaporation in the case of spherical particles of a refractory material in a plasma surrounding. Of the several diffusional mechanisms he examined, he concluded that diffusion thermo (Effect Dufour) had negligible effect on the transfer equations, while thermal diffusion (Effect Soret) had only a small effect.

Borgianni et al. (1969) and Capitelli et al. (1970) studied the decomposition of metal oxides in induction plasmas. It was assumed that the decomposition process was heat transfer controlled, and the reduction in heat transfer due to mass transfer was obtained from the heat transfer result by the use of the relationship

$$h' = h \frac{\ln(1 + \Delta H_v / \Delta H_r)}{(\Delta H_v / \Delta H_r)} \quad (1)$$

The ratio $\Delta H_v / \Delta H_r$ will be recognized as a modified Spalding transport number. Values of h'/h ranged between 0.47 and 0.70 for the large temperature differences encountered.

Rains and Kadlec (1970) studied the thermal decomposition of alumina and used the familiar Ranz and Marshall equation

$$Nu = 2.0 + 0.6 Re^{0.5} Pr^{0.33} \quad (2)$$

to predict the degree of decomposition on the assumption of heat transfer control. Predicted values were about twice those actually obtained; this was due in part to neglecting the influence of mass transfer on heat transfer.

Work on evaporation into high temperature surroundings by Pei et al. (1962) and by Narasimhan and Gauvin (1967) has shown that in the case of combined natural and forced convection heat transfer, the transfer processes may become quite complex depending on whether the bulk flow is opposed to, or combined with, the direction of gravity. The parameter Gr/Re^2 has been shown to be of fundamental importance in describing such systems. In the case of aiding flow, natural convection can usually be

neglected at $Gr/Re^2 < 0.2$, while for $Gr/Re^2 > 80$ forced convection is of little importance.

In a recent theoretical study by Hoffman and Ross (1972), the influence of the surface mass flux on heat transfer was characterized by the Spalding transport number modified for heat transfer by radiation to the evaporating sphere; that is

$$B' = (C_p \Delta T) / (\lambda - q_r / \dot{m}) \quad (3)$$

It was found that the effect of the Spalding number on the transfer rate was virtually independent of Reynolds number. The model was found to be in good agreement with reliable experimental correlations in the Reynolds number range $20 < Re < 500$ for the case of no mass flux, and with a number of analytical shielding expressions in the case of mass transfer.

Finally, the effect of particle geometry on combined heat and mass transfer of stationary and moving particles has been studied by Pasternak and Gauvin (1960, 1961).

KINETICS OF SOLID STATE REACTION

Three main types of models have been developed for the treatment of solids-gas kinetics; they are the homogeneous model attributed to Walker et al. (1959), the shrinking core model of Yagi and Kunii (1955), and generalized models which include each of these two as special cases. Examples of the latter approach are the zone reaction model of Ishida and Wen (1968) and the structural model of Szekely and Evans (1970).

The choice of an appropriate model depends largely on the reaction and physical conditions involved. The isothermal shrinking core model has found considerable application in decomposition reactions, although it has been shown by Narisimhan (1961) that the decomposition of calcium carbonate may be heat transfer controlled. Hills (1967, 1968) has shown that the kinetic data obtained by applying a shrinking core model may be misinterpreted, and that a reaction rate linear with time and a high apparent activation energy may be due to heat and mass transfer effects. Maru et al. (1969a,b) successfully applied an isothermal, shrinking core model to the thermal decomposition of molybdenum disulfide and sesquisulfide in a vacuum system in the temperature range 1190° to 1440°C . In the case of molybdenum disulfide decomposition, these authors formulated a two-stage reaction model in which decomposition to the sesquisulfide was followed by decomposition to the metal. The equilibrium pressure of sulfur was assumed to exist at each reacting interface, and the overall rate of reaction was controlled by the diffusion of sulfur vapor through the two product layers. The model was solved analytically for the reaction of disklike pellets and was found to fit their kinetic data satisfactorily.

In the present study, rates of reaction of spherical pellets were measured. Since microscopic examination of partially reacted specimens revealed the presence of two distinct phases of Mo and MoS_2 only (the sesquisulfide being present in very small quantity), the overall reaction was approximated by a single-stage, shrinking core model, based on mass transfer control of the sulfur through the reacted shell by a pseudo solid state diffusion governed by an effective diffusivity D_e . Assumptions were: (1) isothermal particle, (2) spherical symmetry, (3) quasi steady state, (4) no volume change on reaction, and (5) the sulfur pressure at the particle surface is small and not a function of time. The reaction at the spherical surface with radius r_1 is given by

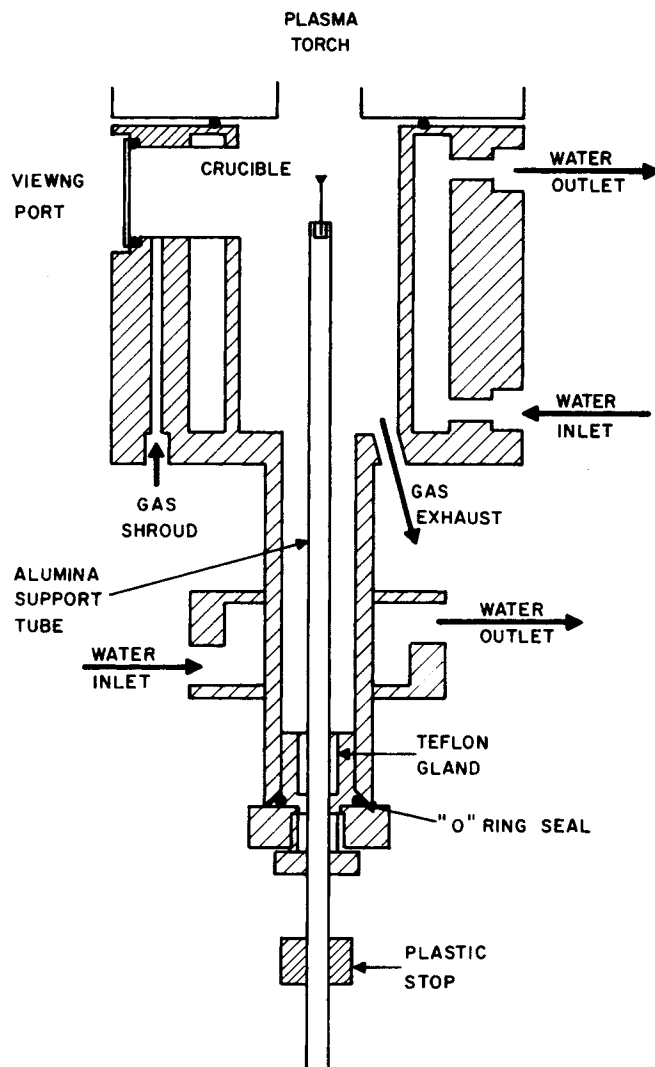
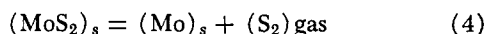


Fig. 1. Schematic drawing of reactor

The model has been developed in detail elsewhere (Munz, 1974) and leads to a time vs. conversion curve of the form

$$t/\tau = 1 - 3(1-x)^{2/3} + 2(1-x) \quad (5)$$

where x is the fractional conversion to molybdenum and is given by

$$x = (W_o - W) (M_{\text{MoS}_2}) / (W_o M_{\text{S}_2}) \quad (6)$$

and τ is the time taken for complete conversion which is given by

$$\tau = (r_o^2 \rho RT) / [(D_e(p_1 - p_o) M_{\text{MoS}_2})] \quad (7)$$

EXPERIMENTAL

Apparatus

The apparatus used in these experiments consisted of an induction plasma torch (TAFA model 56, diameter of exit nozzle = 25.4 mm), with accompanying power supply and control console and the single particle reactor system. High purity argon was used in this work.

The reactor stationary particle was designed specifically to study the kinetics of heterogeneous reactions of a single stationary particle in the tail flame of an induction plasma. A schematic drawing is given in Figure 1. The reaction chamber consisted of a water cooled brass tube 50 mm in diameter and 100 mm long. The effective length of the chamber could be increased further by the installation of one or two water cooled flanged tubes of the same diameter and 25 and/or 38 mm in length. A single window was provided for photography, visual

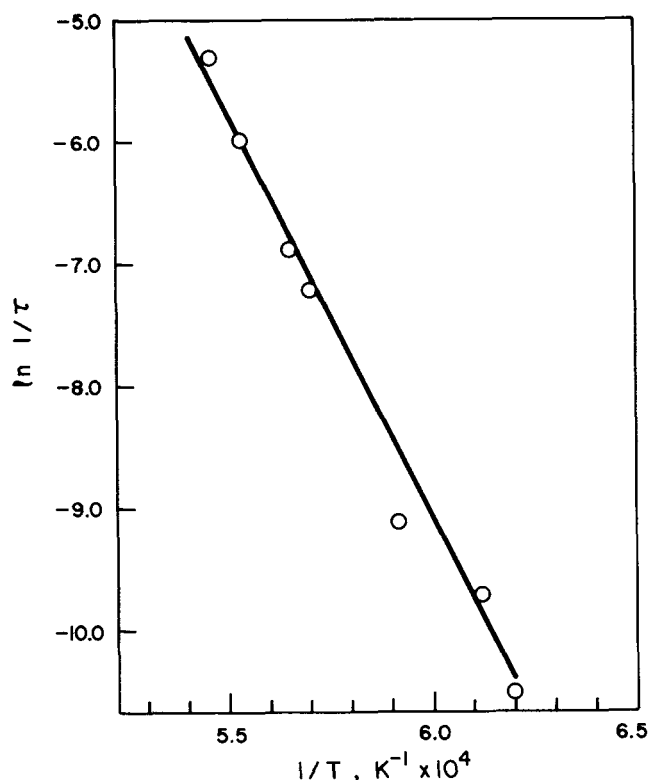


Fig. 2. Arrhenius plot of solid state reaction, sphere diameter = 3.2 mm.

observations, and temperature measurements by optical pyrometry. A shroud of argon prevented the condensation of reaction products on the window and could also be used to purge the reactor before experiments.

The lower part of the reactor housed the particle support system. This region was also water cooled and provided a protected environment for the particle while steady plasma conditions were being obtained. The particle itself was supported on a miniature crucible which was mounted on the top of a 300 mm long alumina tube. The tube was held in an O ring and teflon sliding seal which allowed the entire assembly to be swiftly and accurately positioned in the plasma flame. The crucibles were of molybdenum and were machined to closely fit the bottom of the particle. The very thin stem (1 mm) of the crucible and the low thermal conductivity of the alumina tube served to effectively insulate the reacting particle from the cold reactor.

Measurement Techniques

The molybdenum disulfide used in these experiments was the technical grade commercial product, purified by solvent leaching to a MoS_2 content of 99.5%.^{*} The natural product consists of thin platelets approximately 20 μm in the largest dimension. Spherical pellets were pressed in a steel mould. The void fraction could be varied from 0.14 to about 0.20 by applying the appropriate pressure. Pellets of higher void fractions were made by pressing mixtures of molybdenite and naphthalene and by subsequently removing the naphthalene in a vacuum oven.

The temperature of the reacting particles was measured by using a disappearing filament optical pyrometer. The unknown and changing emissivity of the particles during reaction did not allow a direct temperature determination to be made. However, molybdenite pellets which had been drilled with black-body holes and which were the same size as the reacting particles were used to accurately determine the reaction temperature at the chosen plasma conditions.

The degree of reaction was measured by weight loss of the particles due to the evolution of sulfur vapor. The weight loss used to calculate the amount of reaction was based on half

TABLE 1. EFFECT OF TEMPERATURE CALCULATED TIMES FOR COMPLETE REACTION PARTICLE DIAMETER = 3.2 mm

Series	τ , s	T , °K	Correlation coefficient	P^*
1	36,000	1,613	0.945	0.01
2	401	1,806	0.972	0.01
3	1,360	1,753	0.952	0.001
4	8,980	1,678	0.996	0.001
5	207,000	1,402	0.898	0.1
6	932	1,769	0.762	0.001
7	213	1,833	0.712	0.01
8	16,600	1,635	0.919	0.001

* P is the maximum probability that this value of correlation coefficient could be due to chance. Values of P greater than 0.02 are often used as a criterion for rejection of data.

the particle weight, since the lower half of the pellet did not react owing to the presence of the crucible, as was shown by x-ray and microscopic analysis, which, incidentally, indicated that the pellets were quite isotropic in their structure.

Procedure

A number of spheres of equal diameter were weighed and reacted for different lengths of time as follows: the particle was mounted in the crucible in the lower cool portion of the reactor which was purged for several minutes to remove any residual oxygen. The torch was then ignited and adjusted to the appropriate conditions. Once the plasma was at steady state, the particle support tube was smoothly moved up to the predetermined reaction position and a stopwatch started. Visual observations and pyrometric measurements were made during the reaction, and in some cases the particle was photographed. The temperature of the particle was observed to change very little during a run. After a predetermined length of time, the reaction was quenched by shutting off the torch and purging the chamber with cold argon until the particle had cooled.

Results

X-Ray Analysis and Microscopic Examination

X-ray diffraction analysis showed that the upper surface of partially reacted pellets was invariably molybdenum. Scrapings below this resulted in mixtures of Mo and Mo_2S_3 and then Mo_2S_3 and MoS_2 . At no time, however, was a layer of the sesquisulphide Mo_2S_3 detected. The central core of the pellet as well as the entire lower hemisphere were always found to be pure MoS_2 , thus supporting a shrinkage core model. These observations were confirmed by microscopic examination of sectioned pellets. It was also observed that at the higher temperatures the pore diameter of the reacted layer increased markedly, a behavior which was also reported by Themelis and Gauvin (1962) during the reduction of Fe_2O_3 . In the case of spheres whose void fractions had been artificially increased to 0.47 by naphthalene, a shrinking core behavior was still observed.

Effect of Temperature

This part of the study was carried out at a fixed void fraction of 0.22 by using eight different temperatures ranging from 1 400° to 1 833°K. Below 1 400°K, the rate of reaction was too slow to allow sufficient conversion for analysis in a reasonable reaction time. At temperatures above about 1 840°K the pellets tended to melt locally. These data were fitted to the single-stage reaction model by least squares to determine τ , the time required for complete reaction at each temperature. A summary of this analysis is given in Table 1. The poorest fit was in Series 5, where the temperature was lowest; the large error here is probably due to the very small conversion obtained in these runs.

The data are plotted in an Arrhenius type of relationship in Figure 2, ignoring the results of Series 5. A least-squares analysis of the remaining data gave an activation energy of 134 ± 4 kcal/mole for the reaction.

Effect of Particle Diameter

A total of 63 individual runs were carried out by using pellets in the particle diameter range 2.32 to 4.95 mm, with a con-

* This purification process by leaching is now in commercial operation (U.S. Patent 3,674,424, Canadian Patents 878,999, 879,000).

TABLE 2. EFFECT OF VOID FRACTION CALCULATED TIMES FOR COMPLETE CONVERSION AT 1,777°K

Diameter, mm	T, °K	Series	Void fraction	τ , s
3.2	1,777	5	0.136	1,420
3.2	1,777	6	0.468	486
5.0	1,667	7	0.136	15,300
5.0	1,667	8	0.468	1,810

stant void fraction of 0.217, and at a particle temperature near 1 600°K. The time taken to produce complete reaction for each series of runs was calculated as in the previous section. These times were corrected to the nominal temperature of 1 600°K by using the apparent activation energy determined in the previous section. Figure 3 is a logarithmic plot of τ vs. particle diameter. The solid line is the regression line for the data, while the two dashed lines represent the error introduced by only a $\pm 1\%$ deviation in the temperature of the reacting particle. A single-stage diffusion control would predict a slope of 2.0, while an external diffusion control model would suggest a value between 1.5 and 2.0. If the reaction rate is governed by a chemical kinetic mechanism, a slope of 1.0 is expected. The regression line gives a value of 2.31 ± 0.65 with a correlation coefficient of 0.783 for ten data points. In view of the considerable uncertainty in this slope attributed largely to uncertainties in temperature, a value of 2 would seem reasonable.

Effect of Void Fraction

The effect of the void fraction was investigated in a series of 66 runs on pellets pressed under various pressures ranging from 2.71 to 6.78×10^8 N/m², at a nominal temperature of 1 777°K. The calculated times for complete conversion are plotted as a function of void fraction in Figure 4. A further 30 runs were made to compare the rate of reaction of the naphthalene based pellets of large void fraction (0.495) with those pressed at 4.06×10^8 N/m². Two different particle diameters (3.2 and 5.0 mm) were used. The times for complete reaction for these runs are given in Table 2.

It is evident from both Figure 4 and Table 2 that the time taken for complete reaction increases markedly as the void fraction of the reacting particle is decreased. From Figure 4 the dependence of τ on void fraction seems linear in the region investigated. It would be expected, however, that as the void fraction is reduced to zero, a different diffusion mechanism would prevail.

DISCUSSION

Error Analysis

A detailed analysis of the errors in the solid state kinetic data is available in Munz's thesis (1974). These may have resulted from individual errors in the measurement of reaction time (small), degree of conversion (maximum of 2.2% for large conversions, increasing to 22% for a conversion of 0.1), and particle temperature (about 1%), as well as from nonuniformities in the individual reacting particles (very minor).

To verify the error predictions obtained from the analysis, a series of eight individual runs was carried out under identical reaction conditions at a constant reaction time of 90 s and a nominal reaction temperature of 1 769°K in order to investigate the magnitude of the experimental scatter in the conversion. The latter showed a mean of 0.428 with a standard deviation of 4.67%, which was in line with the expected error for the system.

Kinetic Model

Generally speaking, it can be stated that considerable scatter is to be expected when gas-solid kinetics are studied under such extreme conditions as were encountered in the present work. The choice of a suitable model to represent the reacting system must be based more on physical observations than on the exact fit of experimental data to a

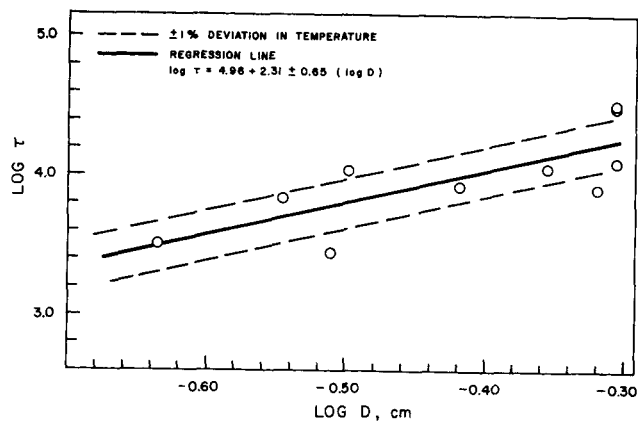


Fig. 3. Influence of particle diameter on time required for complete conversion, $T = 1\ 660^\circ\text{K}$.

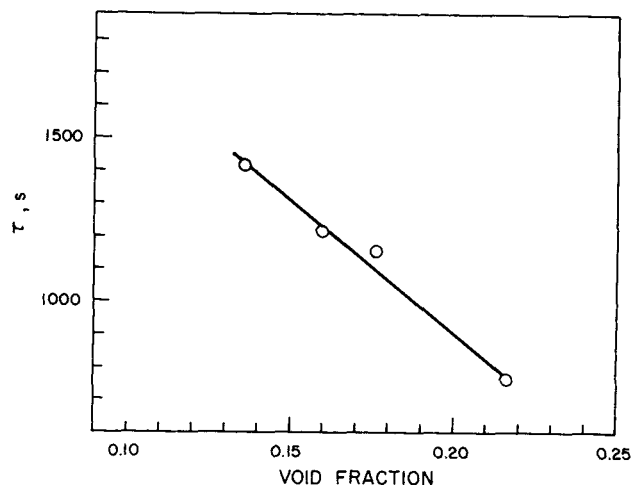


Fig. 4. Influence of void fraction on the time required for complete conversion.

predicted mathematical formulation. It has been shown by Hills (1968) and numerous other authors that even with precise kinetic data, it can be extremely difficult to differentiate between a number of quite different models on the basis of a simple conversion vs. time plot; in the present case, the experimental scatter makes the problem even more difficult.

It has already been pointed out that both microscopic and x-ray examination of partially reacted particles in the present study point strongly to a shrinking core model for the decomposition reaction, while the absence of a sesquisulfide layer justified the use of a single-stage model. Although a two-stage model was applied successfully by Maru et al. (1969b) to their study of molybdenum disks in a vacuum, it does not lead to an analytical solution for a spherical particle. This leads to the important observation that although numerical solutions can always be found in specific cases to fit kinetic data, the lack of morphological information gives these solutions little utility in the treatment of experimental data for other systems or other situations.

It has been suggested by a number of authors that at high temperatures, decomposition reactions of porous solids might well be governed by heat transfer within the reacting solid. If this were to be the case, a decrease in the rate of reaction would be expected as the void fraction of the reacting solid increased, since this would decrease the thermal conductivity of the reacted layer. This is contrary to the effect of void fraction observed in the present work and in that of Maru et al. (1969b).

The apparent activation energy of 134 kcal/mole calculated for the solid state reaction is considerably higher than the value of 86.4 kcal calculated for the same reaction in vacuum by Maru et al. (1969b). The apparent discrepancy does not appear to lie with the model chosen, since a purely empirical plot of log fractional conversion vs. log time gives an activation energy very similar to that obtained by the single-stage reaction model used here. The diffusivities calculated by Maru and co-workers from their kinetic data were later confirmed by direct physical measurements (Maru and Kondo 1973). They have suggested that the measured activation energy was due simply to the change in sulfur vapor pressure above the reacting surface with internal particle temperature. This assumption is not strictly correct, since the effective diffusivity should show a temperature dependency of $T^{1/2}$, as predicted by the mechanism of Knudsen diffusion which prevails in an evacuated system.

An effective diffusivity for diatomic sulfur through the reacted layer of molybdenum has been calculated for the present work by assuming p_0 to be zero and by using the sulfur vapor pressure data of Stubbles and Richardson (1960):

$$p_1 = \exp(18.32 - 43130/T) \quad (8)$$

This results in a rather anomalous temperature dependency of

$$D_e = 0.191T \exp(31.0 - 24300/T) \quad (9)$$

This result cannot be due to the temperature dependency of Knudsen diffusion but may be explained by changes in the reacted layer structure with temperature. Microscopic examination of shells resulting from the lower temperature reactions showed a much finer pore structure (similar to the starting material), while spheres which were reacted at higher temperatures showed a much more open structure. Themelis and Gauvin (1962) observed similar changes in porosity of the iron product layer in their study of the reduction of iron oxide spheres by hydrogen. The particles reacted in vacuum at much lower temperature conditions by Maru and co-workers apparently underwent no great physical change (Kondo, 1971). Moreover, the free energy data of Stubbles and Richardson (1960) which were used to calculate the partial pressure of sulfur at the reacting surface were measured in the temperature range 1123° to 1473°K and were here extrapolated to the temperature range 1635° to 1833°K for the above calculations; computations based on these data must therefore be treated with great reserve.

The influence of void fraction on the effective diffusivity was fitted to a linear form and incorporated into Equation (6) to give

$$D_e = (0.978\epsilon - 0.0210)T \exp(13.0 - 24300/T) \quad (10)$$

The experimental results concerning the influence of particle diameter on the reaction rate show considerable scatter due to previously discussed difficulties encountered in accurate temperature measurement and control. The relation between particle size and reaction rate is, however, consistent with a reaction controlled by the diffusion of sulfur through the reacted molybdenum layer.

A number of computations were made in an attempt to predict the concentration of sulfur in the boundary layer surrounding the reacting particles in the solid state. The results of these calculations were quite approximate owing to a lack of detailed knowledge of the local plasma temperature and velocity in the vicinity of the particles as well as the lack of a reliable correlation for mass transfer which is applicable to transfer at low Reynolds numbers in the presence of very high temperature gradients. They

indicated, however, that the very initial stages of the reaction may be controlled by external mass transfer. This is qualitatively confirmed by the observation of dense clouds of sulfur which accompany the very early stages of reaction.

MOLTEN STATE REACTION

External Heat Transfer Control Model

In this model, it is assumed that the rate of molybdenite decomposition is entirely governed by the rate of heat transfer to the reacting particle. A heat balance on the reacting upper hemisphere* of the particle in quasi steady state may be written as

$$\begin{aligned} Q_{\text{convection from plasma}} + Q_{\text{radiation from plasma}} \\ - Q_{\text{radiation from particle}} - Q_{\text{conduction from particle}} = Q_{\text{reaction}} \end{aligned} \quad (11)$$

In the Reynolds number range of 90 to 145 encountered in this work, convection heat transfer to the particle will be largely of the forced convection type. As previously stated, the radiant flux from the optically thin plasma to the particle will be negligible. It should be further noted that at steady plasma conditions and constant particle and crucible temperature, the left-hand side of Equation (11) is constant.

The fractional conversion of the upper hemisphere at any time is given by Equation (6). From a heat balance on the particle

$$Q_{\text{reaction}} = (\Delta H_r' W_o / M_{\text{MoS}_2}) dx/dt \quad (12)$$

which may be integrated to

$$x = [(Q_{\text{reaction}} M_{\text{MoS}_2}) / (\Delta H_r' W_o)] t \quad (13)$$

A plot of conversion vs. reaction time should thus be linear with a slope of

$$K = (Q_{\text{reaction}} M_{\text{MoS}_2}) / (\Delta H_r' W_o) \quad (14)$$

EXPERIMENTAL

Procedure

The experimental work comprised two parts. The first consisted of nine series of 66 runs at different plasma conditions and a constant sphere diameter of 3.2 mm. The experimentally measured particle weight loss, and hence calculated rates of reaction, were used to determine the nature of the conversion vs-time relationship for the reacting hemisphere. In the second part, particles with diameters ranging from 3.1 to 4.6 mm were reacted, and the rates of reaction were compared with predicted rates of heat transfer to the particles.

The mean temperature of the plasma jet required for heat transfer calculation was measured calorimetrically.

The procedure adapted from the first part was hampered by severe experimental difficulties in this part of the work. The first concerned the molybdenum crucibles holding the reacting pellets. Molybdenum is soluble in molten MoS_2 , and no inert material of construction was available. A solution to this problem was to react upper hemispheres to only about 85% conversion, and in this way the lower hemispheres remained solid, thus protecting the crucible. Some exploratory runs were also carried out on thick disklike pellets to observe the last stages of the reaction. A second problem was the lack of data on the emissivity of liquid MoS_2 . Since a blackbody hole could not be used in this case, only brightness temperatures could be measured. However, since emissivity is not a strong function of temperature, differences in particle temperature could be accurately determined.

* The lower hemisphere is protected by the crucible (which prevents sulfur evolution) and does not react.

Results

Visual and Photographic Observations

The reaction in the molten state consisted essentially of three stages. As the pellet was first exposed to the plasma flame, a thick cloud of sulfur vapor was evolved, as a result of the rapid decomposition of the surface layer. Then, within a short time (less than 10% of the reaction time), the entire top surface of the sphere melted. This stage was accompanied by pronounced internal evolution of sulfur. Although the average shape of the reacting particle during this stage of the reaction remained spherical, its surface was in constant motion as bubbles of sulfur rose to the surface and burst. Occasionally, tiny droplets of liquid were ejected from the surface. The last stage of the reaction consisted of a rapid crystallization of molybdenum from the molten mass. This occurred when conversion was very nearly complete and was observed only when thick disklike samples were used.

X-Ray Analysis and Microscopic Examination

A number of partially reacted pellets were examined by using x-ray powder diffraction. They were found to consist of two layers: a hard consolidated upper crust which had been melted and a soft friable lower portion which remained unreacted and consisted only of MoS_2 . The upper portion of the pellets was homogeneous and contained MoS_2 , Mo_2S_3 , and Mo. The amount of MoS_2 decreased with reaction time, and at near total conversion only Mo was found.

Microscopic examination of sectioned, partially reacted pellets showed an upper layer which was quite hard and brittle and appeared quite uniform in structure. It contained large numbers of spherical cavities which were probably due to bubbles of sulfur which had been frozen into the liquid material as the reaction was quenched. The lower section of the pellet consisted of a soft layer with much finer, angular, pore structure which was identified as unreacted molybdenite and was identical in every way to the unreacted starting material. In the stage of reaction, the upper portion of the pellets became definitely metallic in appearance; although the material was quite porous, the pores were no longer spherical but were interconnecting.

Quantitative Data

For the 66 constant diameter (3.2 mm) runs, the conversion vs. time data are plotted in Figure 5. The temperatures reported on this Figure 5 are the temperatures attained by a molybdenum blank sphere with a blackbody hole, in the same location and at the same plasma conditions as the reacting MoS_2 particle. This temperature is indicative of the rate of heat transfer to the reacting pellet. On the other hand, the temperature of the reacting MoS_2 in the molten state, as measured by the optical pyrometer, was essentially the same for all runs and can reasonably be assumed to be very close to the melting point of MoS_2 , or 1923 K.

A regression of $\log x$ on $\log t$ was used to determine the functional dependence of x on t . The regression coefficient for each series was then weighted by the number of runs in the series, and the best average slope was calculated to be 1.04 ± 0.18 which gives a relation of the form which agrees well with the external heat transfer control model. Only two of the lines are shown in Figure 5.

The remainder of the runs were performed with spheres of different diameter under a variety of plasma conditions. Figure 6 shows the temperature of the molybdenum blank spheres and the brightness temperatures* of the reacting MoS_2 pellets as a function of the applied plate power (all other operating parameters being held constant) for spheres 4.1 mm in diameter. It is important to note that the temperatures of the reacting particles remained essentially constant at all power levels, while the inert molybdenum spheres exposed to identical operating conditions increased in temperature as the power was increased. The results for other sphere sizes were similar.

Energy Balance on Molten State Reaction

An attempt was made to compare the energy gained by the reacting particle to that consumed in reaction by using the kinetic results obtained with spheres of various diameters. In all

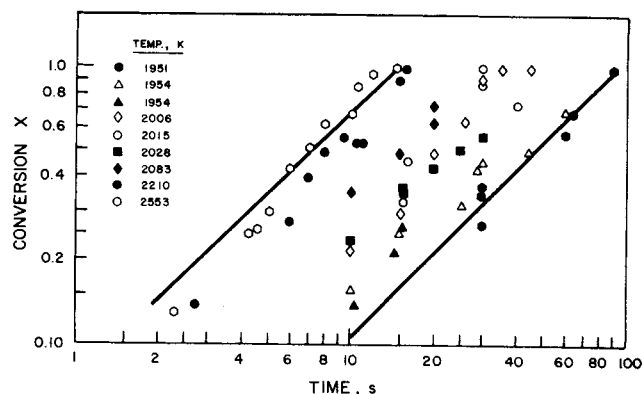


Fig. 5. Liquid state kinetics results, $D = 3.2$ mm.

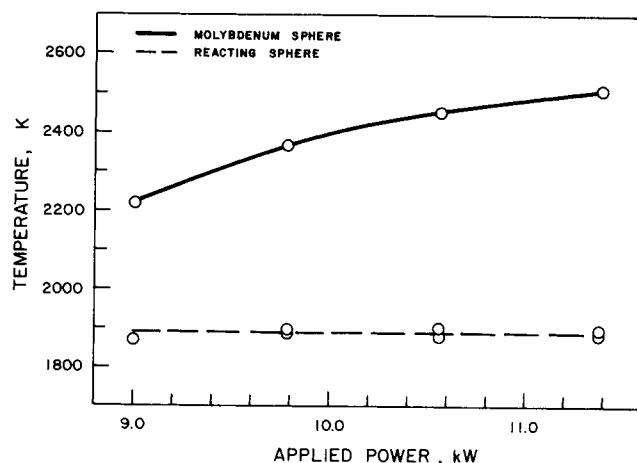


Fig. 6. Comparison of inert molybdenum and reacting particle temperatures at different plasma power levels, Series 10, 20 mm below nozzle, $D = 4.1$ mm, argon flow = 1.44 g/s.

these runs, the reaction rate was measured as a function of plasma power, with all other conditions remaining constant.

The energy balance on the system is expressed in Equation (11). It has already been mentioned that, in this equation, the radiation from the plasma is negligible in view of the very low emissivity of argon. The radiation and conduction from the particles cannot be evaluated exactly but will remain constant throughout the series of runs, since the particle and crucible temperatures remained constant.

The heat taken up by reaction may be calculated from the relationship

$$Q_{\text{reaction}} = (W_0 \Delta H_r K) / (2M_{\text{MoS}_2}) \quad (16)$$

for each series of runs. Here K is the molten state rate constant with units of s^{-1} , and the division by two is due to the fact that only the top half of the sphere reacted. The heat of reaction of molybdenite to molybdenum metal and sulfur was calculated from the data of O'Hare et al. (1970) and Fredrickson and Chasanov (1971). The temperature of the reacting pellet was constant throughout and must have been close to 1923°K, the melting point of MoS_2 at atmospheric pressure, in view of the physical situation. It is worth noting that the exact value of the temperature of the particle is only of minor importance in this discussion, since the heat of reaction is only a weak function of temperature.

The remaining term in Equation (11), namely the heat transferred to the reacting upper hemisphere from the plasma, may be estimated from a correlation of the type

$$Nu = a + b Re^{1/2} Pr^{1/3} \quad (17)$$

which must be corrected for the effects of mass transfer on heat transfer as well as the fact that only transfer to the front half of the sphere is considered. The temperatures and velocities of

* These have not been corrected for emissivity and are thus below 1,923°K.

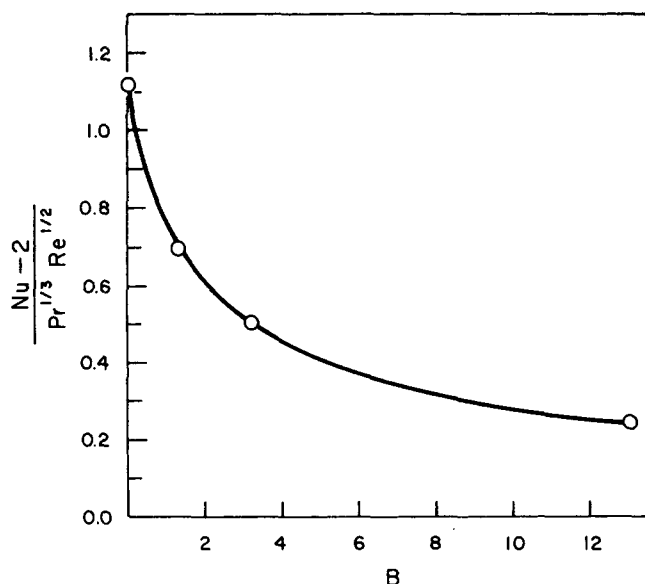


Fig. 7. Influence of mass transfer on heat transfer to leading hemisphere, from Hoffman and Ross (1972).

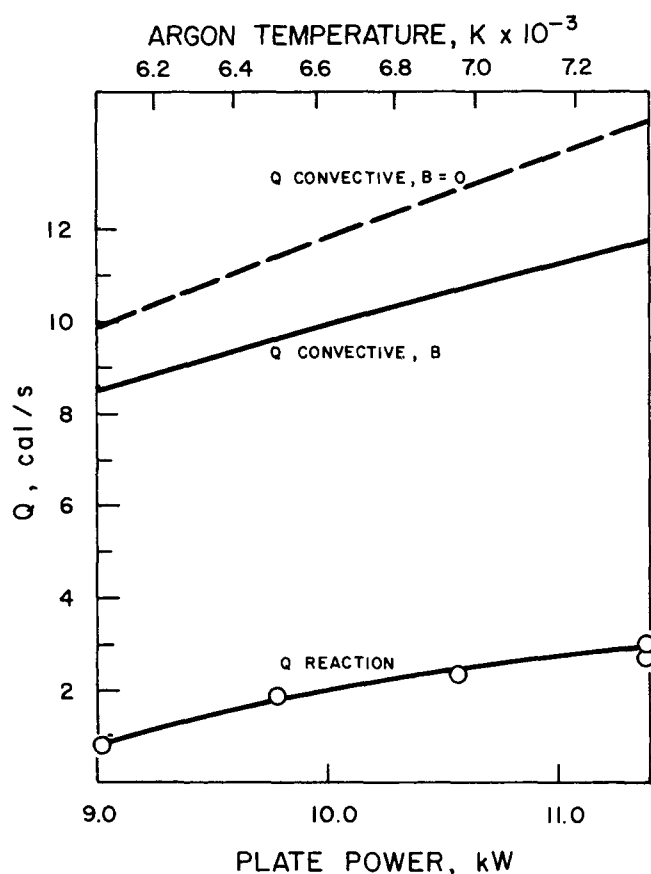


Fig. 8. Comparison of convective heat transfer to reacting particle with heat consumed by reaction, Series 10, 20 mm below nozzle $D = 4.1$ mm, argon flow = 1.44 g/s.

the plasma jet at the position of the reacting particles were calculated by using first the results of the experimental calorimetric study reported by Munz (1974) to obtain mean values and then the predictions of Boulos and Gauvin (1974) to predict centreline conditions.

Reynolds and Prandtl numbers were based on the arithmetic mean film temperature. The Prandtl number was constant at 0.67 in the entire temperature range encountered; Reynolds numbers ranged from 90 to 145 but varied by only 9% within a series of runs.

The predictions of Hoffman and Ross (1972) were then applied to correct both for the influence of mass transfer and the increased heat transfer to the front half of the sphere. The Spalding transport number given in Equation (3) was modified to neglect the radiation term (since this is to be treated separately) and to replace the latent heat by the heat of reaction. This modified Spalding transport number varied from 0.389 to 0.518. The relation of Hoffman and Ross for the local values of the Nusselt number in the presence of mass transfer was graphically integrated to determine the average Nu over the upper hemisphere as a function of B ; this relation is shown in Figure 7 and was used to compute the rate of convective heat transfer to the reacting particle as a function of plate power and the corresponding mean argon temperature at the nozzle exit. A typical result is shown in Figure 8 for the Series 10 of runs. Also shown on this figure are the rates of heat transfer by convection in the absence of mass transfer ($B = 0$) and Q_{reaction} . The difference between the two upper curves reflects the effect of mass transfer on heat transfer and shows that this effect is temperature dependent. It is significant that the two lower curves are very nearly parallel, as they should be since their difference represents the sum of the radiation and conduction from the particles, which are both temperature independent.

DISCUSSION

As has been previously mentioned, the temperature of the reacting liquid could not be determined absolutely owing to its unknown emissivity. The apparent temperature of all reacting particles was, however, constant within the precision of the optical pyrometer for all particles sizes and plasma conditions investigated. This fact, as well as the good fit of the experimental data to the heat transfer control reaction model, indicates that the reaction in the molten state is heat transfer controlled. It was also observed that the contribution to the overall conversion of the initial solid state reaction was small. The violent bubbling observed during the molten state reaction, as well as the homogeneous nature of the reacted product, indicates that the liquid phase is well mixed during most of the reaction. Additional exploratory studies with disk-like particles showed that the final crystallization to molybdenum metal is very rapid and occurs only in the very last stages of reaction. Following this crystallization, the particle temperature rose rapidly to a new steady state value.

The calculations of convection heat transfer to the reacting particles were based on the velocity and temperature profiles calculated by Boulos and Gauvin (1974) at a distance from the nozzle at which both free and confined jets are similar. The mean plasma temperatures and velocities which were fitted to their flow calculations are considered accurate to about 5%.

At the relatively low temperatures used in this work, recombination of ions and electrons was not expected to contribute to heat transfer. It is quite conceivable that a temperature ratio or gas property ratio correction should have been incorporated in Equation (17) to account for the high temperature differences involved. In the absence of an empirical equation suited to the present experimental conditions, the use of such a correction was not considered appropriate. Similarly, natural convection effects could be ignored, since the value of the parameter Gr/Re^2 was calculated to be of the order of 10^{-5} in all cases. The correlation by Hoffman and Ross (1972) which was used to account for the influence of mass transfer on heat transfer has admittedly not been tested under plasma conditions but agrees well with other correlations under less severe conditions. A number of additional complications might be expected to interfere with an accurate prediction of the convective heat transfer term. For example, the surface of the sphere was in constant motion owing to the evolution

of vapor bubbles, and thus the diameter of the particle was not constant throughout.

In spite of these numerous difficulties and uncertainties, the difference between the calculated convective heat transfer and the heat taken up by reaction remained remarkably constant, as shown in Figure 8. From these calculations, it may also be observed that mass transfer has a significant effect on heat transfer in reacting plasma systems. This would be even more pronounced in the case of simple evaporation, where B would reach much greater values. It is also interesting to note that, in the case of a larger stationary reacting particle, most of the heat given to the particle by the plasma is lost again by radiation, either directly or by conduction to the crucible and radiation from the latter. If reactions are to be studied at higher temperatures, either small particles or radiation shields must be added.

An extension of this study over a wider range of Reynolds numbers or with gases having different transport properties would certainly have been of interest. However, the use of higher gas velocities in the present equipment by decreasing the torch nozzle size would have resulted in severe particle erosion problems as well as high blockage ratios. Moreover, the use of another plasma gas was not feasible, since only helium in addition to argon is inert to molybdenum, and the induction torch does not operate satisfactorily with helium. Finally, it is felt that more could be gained from a heat transfer study involving only vaporization, where the system properties are better understood. Under these conditions the radiation terms could be independently evaluated.

A word should be said regarding the importance of the molten state results with respect to the reaction of small freely entrained molybdenite particles. Although a large portion of the heat transferred to large particles is lost as radiation, these losses become much less relevant for particles approaching, say, 20μ in diameter, which would be the size of naturally occurring MoS_2 . Thus, although the liquid emissivity is an important parameter in predicting the rate of reaction of large particles, it becomes a minor consideration in the modeling of small particles. Since the Reynolds numbers of freely entrained particles will be much smaller, the use of a Nusselt number of 2 might be quite adequate as a first approximation, although this should be corrected for mass transfer effects.

ACKNOWLEDGMENT

This work forms part of a continuing program of research carried out by the Plasma Technology Group in the Department of Chemical Engineering of McGill University, with the financial assistance of a Special Project Grant from the National Research Council of Canada.

NOTATION

B	= modified Spalding number
C_p	= heat capacity, $\text{L}^2\text{t}^{-2}\text{K}^{-1}$
D	= sphere diameter, L
D_e	= effective diffusivity, L^2t^{-1}
Gr	= Grashof number
h	= heat transfer coefficient, $\text{Mt}^{-3}\text{K}^{-1}$
K	= reaction rate constant, t^{-1}
M	= molecular weight, M mole $^{-1}$
m	= mass flow rate, Mt^{-1}
Nu	= Nusselt number
P	= probability
Pr	= Prandtl number
p	= partial pressure of sulfur, $\text{M L}^{-1}\text{t}^{-2}$
Q	= rate of heat transfer, ML^2t^{-3}
q_r	= rate of radiant heat transfer, ML^2t^{-3}

R	= gas constant, $\text{M L}^2\text{t}^{-2}\text{K}^{-1}\text{mole}^{-1}$
Re	= Reynolds number
r	= sphere radius, L
T	= temperature, K
t	= time, t
W	= mass, M
W_0	= initial mass, M
X	= fractional conversion
Y	= $1 - 3(1 - x)^{2/3} + 2(1 - x)$

Greek Letters

$\Delta H_r'$	= heat of reaction, $\text{ML}^2\text{t}^{-2}\text{mole}^{-1}$
ΔH_r	= enthalpy change of vapor, $\text{ML}^2\text{t}^{-2}\text{mole}^{-1}$
ΔT	= temperature difference between surface and bulk, K
ϵ	= void fraction
λ	= latent heat of vaporization, L^2t^{-2}
ρ	= density, M L^{-3}
τ	= time for complete reaction, t

Subscripts

0	= outer sphere surface
1	= reaction interface

LITERATURE CITED

- Bhattacharyya, D., and W. H. Gauvin, "The Modeling of a Confined Plasma Jet Reactor," paper presented at the Joint Conference of AIChE-V.G.T., Munich, Germany (Sept. 17-24, 1974).
- Bonet, C., "Etude Théorique de l'Evaporation d'une Particule Sphérique d'un Matériau Réfractaire dans un Plasma Thermique," *Intern. J. Heat Mass Transfer*, **17**, 1559 (1974).
- Borgianni, C., M. Capitelli, F. Cramarossa, L. Friolo, and E. Molinari, "The Behavior of Metal Oxides Injected into an Argon Induction Plasma," *Combust. Flame*, **13**, 181 (1969).
- Boulos, M. I., and W. H. Gauvin, "Powder Processing in a Plasma Jet: Proposed Model," *Can. J. Chem. Eng.*, **52**, 3, 355 (1974).
- Capitelli, M., F. Cramarossa, L. Friolo, and E. Molinari, "Decomposition of Al_2O_3 Particles Injected into Argon. Nitrogen Induction Plasmas of One Atmosphere," *Combust. Flame*, **15**, 23 (1970).
- Charles, J. A., G. J. Davies, R. M. Jervis, and G. Thurstfield, "Processing of Minerals in an Induction-coupled Torch," *Trans. Sect. C. Inst. Min. Met.*, **79**, 54 (1970).
- Chludzinski, G. R., R. H. Kadlec, and S. W. Churchill, "Energy Transfer to Probes in Argon Nitrogen Plasmas," paper presented at AIChE—Instn. Chem. Engrs. Joint Meeting, London, England (1965).
- Clamen, A., and W. H. Gauvin, "Drag Coefficients of Evaporating Spheres in a Turbulent Air Stream," *Can. J. Chem. Eng.*, **46**, No. 2, 73 (1968).
- Fredrickson, D. R., and M. G. Chasanov, "The Enthalpy of MoS_2 to 1 200 K by Drop Calorimetry," *J. Chem. Thermodynamics*, **3**, 693 (1971).
- Hills, A. W. D., ed., *Heat and Mass Transfer in Process Metallurgy*, p. 39, Inst. Min. and Met., London, England (1967).
- , "The Mechanism of Thermal Decomposition of Calcium Carbonate," *Chem. Eng. Sci.*, **23**, 297 (1968).
- Hoffman, T. W., and L. L. Ross, "A Theoretical Investigation of the Effect of Mass Transfer on Heat Transfer to an Evaporating Droplet," *J. Heat Mass Transfer*, **15**, 599 (1972).
- Huska, P. A., and C. W. Clump, "Decomposition of Molybdenite in an Induction Coupled Argon Plasma," *Ind. Eng. Chem., Process Design Develop.*, **6**, No. 2, 238 (1967).
- Ishida, M., and C. Y. Wen, "Comparison of Kinetic and Diffusional Models for Solid-Gas Reactions," *AIChE J.*, **14**, No. 2, 311 (1968).
- Johnston, P. D., "A Measurement of the Lifetime of the $1S_5$ Argon Metastable in Argon at Atmospheric Pressure," *Physics Letters*, **34A**, 7, 389 (1971).
- Katta, S., and W. H. Gauvin, "Local and Overall Heat Transfer to Spheres in a Confined Plasma Jet," AIChE E. Symposium Series No. 131, Heat Transfer: Fundamentals and Industrial Applications, Vol. 69, p. 174 (1973a).

- _____, "The Effect of Local Gas Velocity and Temperature on the Local Heat Transfer to a Sphere in a High Temperature Jet," *Can. J. Chem. Eng.*, **51**, 3, 307 (1973b).
- Kimura, I., and A. Kanzawa, "Experiments on Heat Transfer to Wires in a Partially Ionized Argon Plasma," *AIAA J.*, **3**, No. 3, 475 (1965).
- Kondo, Y., Private communication (1971).
- Kubaneck, G. R., P. Chevalier, and W. H. Gauvin, "Heat Transfer to Spheres in a Confined Plasma Jet," *Can. J. Chem. Eng.*, **46** No. 2, 101 (1968).
- Maru, Y., H. Yoshida, and Y. Kondo, "On the Thermal Decomposition Rate of Molybdenum Sesquisulphide," *Trans. Japan Inst. Metals*, **10**, No. 1, 8 (1969a).
- Maru, Y., K. Ito, and Y. Kondo, *Thermal Analysis*, R. F. Schwenker, P. D. Garn, ed., p. 1291, Academic Press, New York (1969b).
- Maru, Y., and Y. Kondo, "Effective Diffusivity Through a Porous Solid," *Trans. Japan Inst. Metals*, **14**, No. 4, 303 (1973).
- Matsumoto, O., "Formation of Titanium Nitride by Means of a Transferred Arc Plasma Jet," *J. Electrochem. Soc. Japan*, **36**, No. 3, 1953 (1968).
- _____, "Oxidation of Titanium by Means of an Argon Oxygen Plasma Jet," *ibid.*, **37**, No. 4, 200 (1969).
- _____, and Y. Kawai, "Nitriding Reaction of Zirconium by Nitrogen Plasma Jet," *Denki Kagaku*, **40**, No. 4, 271 (1972).
- Munz, R. J., "The Decomposition of Molybdenum Disulphide in an Induction Plasma Tailflame," Ph.D. thesis, McGill University, Montreal, Canada (1974).
- Narasimham, C., and W. H. Gauvin, "Heat and Mass Transfer to Spheres in High Temperature Surroundings," *Can. J. Chem. Eng.*, **45**, 181 (1967).
- Narasimhan, G., "Thermal Decomposition of Calcium Carbonate," *Chem. Eng. Sci.*, **16**, No. 1-2, 7 (1961).
- O'Hare, P. A. G., E. Benn, F. Yu Cheng, and G. Kuzmycz, "A Fluorine Bomb Calorimetric Study of Molybdenum Disulphide," *J. Chem. Thermodynamics*, **2**, 797 (1970).
- Pasternak, I. S., and W. H. Gauvin, "Turbulent Heat and Mass Transfer from Stationary Particles," *Can. J. Chem. Eng.*, **38**, 35 (1960).
- _____, "Fundamental Aspects of Solids-Gas Flow Part IV: The Effects of Particle Rotation," *AIChE J.*, **7**, No. 2, 254 (1961).
- Pei, D. C. T., C. Narasimhan, and W. H. Gauvin, "Proceedings of the Symp. on the Interaction between Fluids and Particles," *Inst. Chem. Engrs. London*, 243 (1962).
- Petrie, T. W., "The Effect of Ionization on Heat Transfer to Wires Immersed in an Argon Plasma," Ph.D. thesis, University of Minnesota (1969).
- Rains, R. K., and R. R. Kadlec, "Reduction of Al_2O_3 to Aluminum in a Plasma," *Metall. Trans.*, **1**, 1501 (1970).
- Rother, W., V. Smolyakov, and K. H. Weiss, "Konvektive Wärmeübertragung in einem Laminaren Stickstoff-Plasma Strahl I," *Beitr. Plasma-Phys.*, **8**, 145 (1968a).
- Rother, W., "Konvektive Wärmeübertragung in einem Laminaren Stickstoff-Plasma Strahl II," *ibid.*, **8**, 157 (1968b).
- Savce, I. G., "Plasma Processes in Extractive Metallurgy," *Proc. Int. Symp. Advan. Ext. Met. Refining*, London, Eng., **241** (1972).
- Scholz, W. G., D. V. Doane, and G. A. Timmons, "Molybdenum by Direct Thermal Dissociation of Molybdenite," *Trans. Metallurgical Soc. AIME*, **221**, 356 (1961).
- Stubbs, J. R., and F. D. Richardson, "Equilibria in the System $\text{Mo} + \text{S} + \text{H}_2$," *Trans. Faraday Soc.*, **56**, 1460 (1960).
- Szekely, J., and J. W. Evans, "A Structural Model for Gas Solid Reactions with a Moving Boundary," *Chem. Eng. Sci.*, **25**, 1091 (1970).
- Themelis, N. J., and W. H. Gauvin, "The Mechanism of the Reduction of Iron Oxides," *Trans. Can. Inst. Min. Met. Eng.*, **65**, 229 (1962).
- Triché, H., C. Butti, and J. Besombes-Vailhe, "Study of Volatilization and Chemical Reaction in the Plasma Torch," *Methodes Phys. d'Anal.*, **4**, No. 4, 379 (1968).
- Waldie, B., "Review of Recent Work on the Processing of Powders in High Temperature Plasmas—Part I, Processing and Economic Studies," *The Chemical Engineer*, **259**, 92 (1972a).
- _____, "Review of Recent Work on the Processing of Powders in High Temperature Plasmas—Part II, Particle Dynamics Heat Transfer, Mass Transfer," *ibid.*, **261**, 188 (1972b).
- Walker, P. L., F. Rusinko, and L. G. Austin, "Gas Reactions of Carbon," *Advan. Catalysis*, **11**, 133 (1959).
- Yagi, S., and D. Kunii, "Studies on Combustion of Carbon Particles in Flames and Fluidized Beds," *Proc. 5th Int. Symp. Combustion*, Pittsburgh, Penn. 1954, 231 (1955).
- Zelikman, A. N., and L. V. Belyaevskaya, "The Melting Point of Molybdenite," *J. Inorganic Chemistry U.S.S.R.*, **1**, No. 10, 2239 (1956).

Manuscript received Feb. 14, 1975; revision received and accepted August 1, 1975.

The Vapor-Liquid Equilibrium of the Hydrogen-n-Butane System at Elevated Pressures

The vapor-liquid equilibrium of the hydrogen-n-butane system was studied at temperatures between 54° and 121°C and at pressures up to 167 atm. The fugacity of hydrogen in the vapor phase was measured directly by using a palladium-silver semipermeable membrane, whereas p-T-x-y data were obtained in a conventional manner.

Henry's constants for hydrogen in n-butane were obtained from the experimental fugacity data without making any assumptions about the vapor phase. Constant-pressure, liquid-phase activity coefficients for both hydrogen and n-butane were calculated and correlated by using a modified van Laar equation.

A. E. Klink is with Merck and Company, Rahway, N.J. 07065. E. H. Amick, Jr. is deceased.

A. E. KLINK,
H. Y. CHEH,
and
E. H. AMICK, JR.

Department of Chemical Engineering and
Applied Chemistry
Columbia University
New York, New York 10027